RESEARCH ARTICLE

Altered executive control network connectivity in anti-NMDA receptor encephalitis

Zhongqin Chen[a], Jintao Zhou[a], Dengchang Wu, Caihong Ji, Benyan Luo (iD) & Kang Wang (iD)

Department of Neurology, The First Affiliated Hospital, College of Medicine, Zhejiang University, Hangzhou, China

Correspondence

Kang Wang, Department of Neurology, The First Affiliated Hospital, College of Medicine, Zhejiang University, Hangzhou, China. Tel: (86) 571 8723 5101; Fax: (86) 571 8722 2061; E-mail: fcwangk1@zju.edu.cn

[a]These authors contributed equally to this work and should be considered co-first authors.

Abstract

Objective: The goal of this study was to examine whether the static functional connectivity (FC) of the executive control network (ECN) and the temporal properties of dynamic FC states in the ECN can characterize the underlying nature of anti-*N*-methyl-D-aspartate (anti-NMDA) receptor encephalitis and their correlations with cognitive functions. **Methods**: In total, 21 patients with anti-NMDA receptor encephalitis past the acute stage and 23 healthy controls (HCs) underwent a set of neuropsychological tests and participated in a resting-state fMRI study to analyse the static FC of the ECN and the temporal properties of dynamic FC states in the ECN. In addition, correlation analyses were performed to determine the correlations between the FC metrics and cognitive performance. **Results**: Patients with anti-NMDA receptor encephalitis past the acute stage showed significant cognitive impairments compared to HCs. In accord with the results of neuropsychological tests, static intrinsic FC alterations and changed dynamic FC metrics of ECN were observed in the patients. Importantly, we observed significant correlations between altered ECN metrics and working memory, information processing speed, executive function performance in the patients. **Interpretation**: Our findings suggest that cognitive impairments in patients with anti-NMDA receptor encephalitis past the acute stage are likely related to altered static and dynamic ECN connectivity. These observations may enhance our understanding of the pathophysiological mechanisms underlying cognitive function in this population.

Introduction

Anti-*N*-methyl-D-aspartate (anti-NMDA) receptor encephalitis is an immune-mediated and treatable brain inflammation characterized by the acute onset of a constellation of symptoms.[1,2] The typical clinical manifestations include loss of consciousness, abnormal behaviour and cognition, speech disorder, memory deficit, abnormal movements, seizures, autonomic dysfunction and central hypoventilation.[3] Approximately 80% of patients showed substantial recovery after timely treatments according to the low modified Rankin Scale (mRS).[3] However, many studies have indicated that cognitive impairments, especially memory deficits and executive function impairments, constitute a major long-term consequence of this disorder, which are also consistent with high density of NMDA receptors within the hippocampus and frontal cortex.[4-6] A former study by our team showed that early administration of intravenous second-line immunotherapy may be associated with more favourable verbal episodic memory outcomes; nonetheless, the patients still exhibited other domains of cognitive impairments of varying degrees, including working memory, information processing speed and executive function.[6]

Exploring the neurophysiological mechanisms underlying cognitive deficits, especially memory impairments in patients with anti-NMDA receptor encephalitis, by using multimodal functional MRI has attracted intensive attention in recent years.[7-9] However, to our knowledge, fMRI studies about other domains of cognitive impairments, such as working memory, information processing speed and executive function are very few in literature, which has limited our understanding of this disease. The impairment of these cognitive functions has made great impact on the patients' study, work and life. It is necessary to pay attention to investigate these cognitive impairments and its mechanism for patients with anti-NMDA receptor encephalitis.

Working memory, information processing speed and executive function tasks in healthy individuals have been shown to engage groups of brain regions, such as the dorsolateral/ventrolateral prefrontal cortex and the lateral parietal cortex, which are integrated in the executive control network (ECN).[10–12] A resting fMRI study based on hard parcellation of large-scale brain network analyses indicated that functional connectivity (FC) changes in frontoparietal networks (i.e. ECN) are impaired and associated with schizophrenia-like symptoms in anti-NMDA receptor encephalitis.[13] However, this study did not focus on whether the ECN changes were related to cognitive function impairments in this population.

In addition, previous studies did not consider the significant dynamic characteristics in the brain network in anti-NMDA receptor encephalitis, as FC was supposed to be constant during resting-state functional MRI scanning. It is noteworthy that resting state FC can vary considerably at different temporal scales.[14–16] Temporal dynamic characteristics can be detected in brain FC by analysing functional MRI signals and such analyses may demonstrate neural mechanisms that cannot be revealed through static resting state FC alone.[15–18] The clinical relevance and potential biomarker applications of dynamic FC have been suggested in clinical studies of epilepsy,[19,20] Alzheimer's disease,[21] Parkinson's disease,[22] schizophrenia[23] and autism.[24] However, to the best of our knowledge, altered FC in the ECN in a dynamic context remains unknown in patients with anti-NMDA receptor encephalitis past the acute stage.

In the present study, we used resting-state fMRI and employed a group-level independent component analysis (ICA) to generate ECN. Then, we compared the static and dynamic FC of the ECN in patients with anti-NMDA receptor encephalitis and healthy controls (HCs). We speculated that abnormal static and dynamic metrics of ECN may exist and may be associated with cognitive performance in patients with anti-NMDA receptor encephalitis. Therefore, we aimed to determine whether static FC of the ECN and the temporal properties of dynamic FC states in the ECN could characterize the underlying nature of anti-NMDA receptor encephalitis and correlate with cognitive functions.

Methods

Subjects

Twenty-one patients with anti-NMDA receptor encephalitis who were hospitalized or referred to the outpatient clinic for further counselling and treatment at the Department of Neurology, First Affiliated Hospital, College of Medicine, Zhejiang University were recruited between July 2016 and December 2019. Demographic and clinical data

of the patients are shown in Table 1. The diagnosis was based on typical clinical features together with the presence of IgG antibodies for NMDA receptors.[2,25] There were no abnormalities in structural MRI for any patient. The assessment was conducted after the acute stage of the disease (at least 6 months after initial discharge from the hospital).

Twenty-three individuals with no history of psychiatric or neurologic disease served as HCs in the experiments. All the patients (8 males, age: 27.48 ± 9.49 years, educational level: 13.52 ± 2.34 years) and HCs (8 males, age: 26.43 ± 5.22 years; educational level: 14.65 ± 1.77 years) were evaluated using neuropsychological assessments and underwent an MRI scan.

All subjects provided written informed consent, and the project was approved by the Ethics Committee of the First Affiliated Hospital, School of Medicine, Zhejiang University.

Neuropsychological assessment

A set of comprehensive neuropsychological tests were used, which covered working memory (digit span test, DST), verbal episodic memory (Chinese auditory verbal learning test, CAVLT), executive function (Stroop color and word test) and information processing speed (symbol digit modalities test, SDMT). We also used self-rating anxiety scale (SAS) and self-rating depression scale (SDS) to evaluate emotional state.

MRI data acquisition

All subjects were scanned with a Siemens MAGNETOM Prisma 3 T scanner (Siemens, Erlangen, Germany) at the Center for Brain Imaging Science and Technology, Zhejiang University using the standard setup for clinical studies with a 20-channel phased array head coil. Foam padding was used to minimize head movement, and earplugs were used to reduce scanner noise. High-resolution three-dimensional (3D) T1-weighted MRI scans were collected using a magnetization prepared rapid gradient-echo sequence (repetition time = 2300 msec, echo time = 2.32 msec, inversion time = 900 msec, flip angle = 8°, field of view = 240 × 240 mm², matrix size = 256 × 256, 192 slices, slice thickness = 0.90 mm). Resting-state fMRI was performed using an echo-planar imaging sequence (repetition time = 1000 msec, echo time = 34.0 msec, flip angle = 62°, field of view = 230 × 230 mm², 52 slices, slice thickness = 2.50 mm, acquisition time = 5 min, 300 volumes). All the subjects were instructed to lie still with their eyes closed while remaining awake during the resting-state fMRI scans. The framework of characterizing and static dynamic ECN connectivity is shown in Figure S1.

Table 1. Demographic and clinical data of patients.

Patient	Sex	Age	Igg NMDA receptor antibodies (CSF titre)	Symptoms		Hospital stay, (months)	mRS Score		Time between initial discharge and data acquisition (months)
				Initial	Total		Before treatment	At study time point	
1	F	24	1:32	Behaviour	LOC, dyskinesia, seizure, behaviour, cognition	1.2	5	0	18.5
2	F	22	1:32	Behaviour, seizure	LOC, dyskinesia, seizure, behaviour, cognition	1.1	5	0	6.5
3	M	28	1:32	Behaviour, dyskinesia	LOC, dyskinesia, seizure, behaviour, cognition, autonomic instability	1.2	5	1	9.3
4	M	31	1:32	Seizure, LOC	LOC, dyskinesia, seizure, behaviour, cognition, autonomic instability	1.4	5	0	21
5	F	15	1:32	Dyskinesia, seizure	Dyskinesia, seizure, behaviour, cognition	1.2	4	1	6.1
6	F	25	1:32	Behaviour, seizure	LOC, dyskinesia, seizures, behaviour, cognition	1.2	5	0	8.3
8	F	16	1:10	Behaviour	Seizure, behaviour, cognition	1.2	4	0	10.6
9	F	29	1:3.2	Behaviour	LOC, behaviour, cognition	0.7	4	0	6.5
10		48	1:32	Behaviour, seizure	Seizure, behaviour, cognition	1.1	4	1	8.5
11	F	33	1:10	dyskinesia, Cognition	Dyskinesia, behaviour, cognition	0.9	4	0	12.1
12	F	18	1:32	Behaviour	dyskinesia, seizure, behaviour, cognition	1.3	4	0	6.7
13	F	18	1:32	Behaviour, LOC	LOC, dyskinesia, seizure, behaviour, cognition	0.9	5	1	13.3
14	M	19	1:10	Seizure, behaviour	LOC, dyskinesia, seizure, behaviour, cognition	2.1	5	1	10.3
15	F	40	1:10	Seizure, behaviour	Seizure, behaviour, cognition	0.8	4	1	7.2
16	M	22	1:32	Behaviour	LOC, dyskinesia, seizures, behaviour, cognition	0.8	4	0	23.9
17	F	41	1:10	Seizure, behaviour	LOC, seizure, behaviour, cognition, autonomic instability	1.2	5	1	16
18	F	34	1:32	Behaviour, cognition	LOC, dyskinesia, seizures, behaviour, cognition, autonomic instability	26	5	0	36.2
19	F	24	1:32	Seizure, behaviour,	Seizure, behaviour, cognition	1.3	5	0	23.2
20	M	21	1:32	Behaviour, seizure	LOC, seizure, behaviour, cognition	1.3	4	0	21.5
21	M	44	1:10	Behaviour	Seizure, behaviour, cognition	1.2	4	1	11.2
22	M	25	1:32	Behaviour, seizure	LOC, dyskinesia, seizures, behaviour, cognition, autonomic instability	1.6	5	0	47

CSF, cerebrospinal fluid; LOC, loss of consciousness; mRS, modified Rankin scale; NMDA, *N*-methyl-D-aspartate.

Resting-state fMRI data preprocessing

Resting-state fMRI data were preprocessed using the Graph-theoretical Network Analysis Toolkit (GRETNA)[26] based on SPM12 (http://www.fil.ion.ucl.ac.uk/spm/software/spm12). The processing included the following steps. First, the first 20 volumes of functional images were discarded to allow the longitudinal magnetization to reach a steady state and to acclimate the participant to the scanning noise, and then head motion correction were performed. Head motion did not exceed 3.0 mm of maximal translation (in the x, y or z direction) or 3.0° of maximal rotation throughout the course of scanning in any of the subjects. Second, 3D T1 images were aligned to an individual averaged functional image and subsequently spatially normalized to the MNI template ($3 \times 3 \times 3$ mm) using diffeomorphic anatomical registration through exponentiated lie algebra (DARTEL) algorithm for spatial normalization. Third, the resulting images were spatially smoothed using a 6-mm full width at half-maximum (FWHM) Gaussian kernel. The acquired smoothed data were utilized in ICA.

Identification of ECN

Group spatial ICA was adopted to decompose all preprocessed data into independent components (ICs) using GIFT software[27] with the following steps. First, a two-step principal component analysis was applied to reduce the data into 34 independent components, using the minimum description length criterion.[28] The reliability of the infomax ICA algorithm's estimations were evaluated through a comparison against 20 iterative estimates using ICASSO implemented in GIFT.[29] Second, we applied a spatially constrained approach called group information-guided ICA[30] to perform back reconstruction of participant-specific spatial maps and corresponding time courses. Third, of the 34 independent components, 5 independent components of the ECN were selected by visual comparisons with previously defined maps.[31,32] No network templates were applied. The selected ECN is shown in Figure 1. Finally, additional postprocessing steps were performed on the time courses of the ECN as follows. The time courses of ECN were detrended (linear, quadratic and cubic trends). Then, the
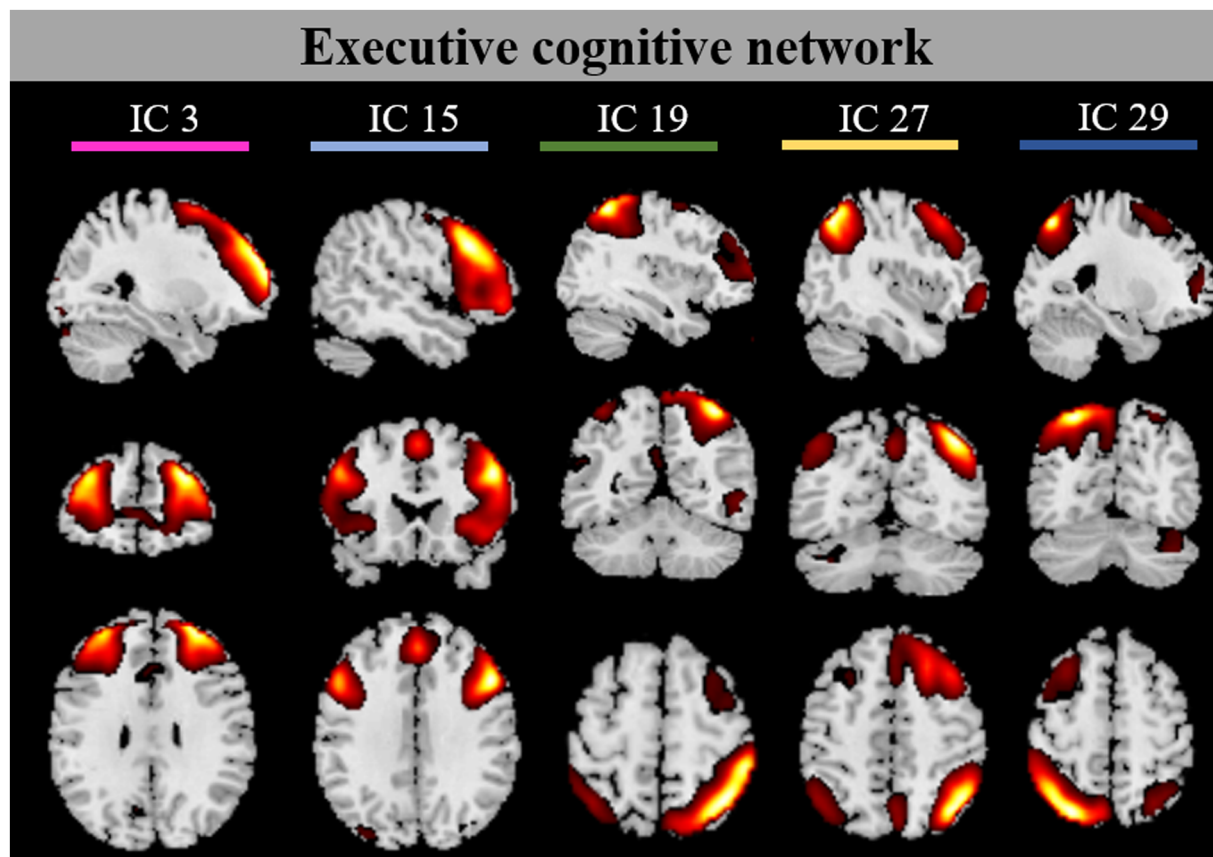

Figure 1. The five independent components of executive control network identified by a group ICA. IC 3, mainly located in the ventrolateral prefrontal cortex; IC 15, mainly located in the dorsolateral and medial prefrontal cortex; IC 19 and 27, mainly located in the right frontoparietal executive network; IC 29, mainly located in the left frontoparietal executive network; ICA, independent component analysis.

resulting images were despiked, outliers were detected, and finally, they were low-pass filtered with a cutoff frequency of 0.15 Hz.

Static ECN connectivity analysis

We performed pairwise Pearson correlations to create a static FC matrix of ECN by using the postprocessed time courses between the independent components over the entire scan; these were then converted to *z*-values using Fisher's *z*-transformation. Then, we used two-sample *t*-tests to compare the differences in ECN correlation values between patients and HCs. We used a threshold of $p < 0.05$ and applied a false discovery rate (FDR) correction to each analysis to correct for multiple correlation comparisons. In addition, to explore the FC between brain regions within the ECN, five region of interest (ROI) spheres (radius: 6 mm) were built around peak activations in respective five ICs of ECN. Then seed-based FC analysis was performed.

Next, we calculated the Pearson correlation between abnormal ECN connectivity and executive control performance in patients and HCs, respectively, to explore the potential relationship. The correlation analyses were performed using SPSS 16.0 for Windows (SPSS Inc., Chicago, IL).

Dynamic ECN connectivity

The processing used the dynamic FC toolbox in GIFT to perform the following steps. First, we used a sliding window approach to explore time-varying changes in FC in five independent components of the ECN during resting-state fMRI scans. The window size was 30 TR convolved with sigma 3 TR of Gaussian, based on previous reports that a window size range of 30 sec to 1 min is a reasonable choice for obtaining dynamic patterns in FC.[15,16,33] The window was moved in steps of 1 TR, resulting in 250 consecutive windows across the entire scan. A covariance matrix with windowed data was calculated to measure the dynamic FC between the components in the ECN. Then, the changes in FC between components in the ECN for each participant as a function of time were estimated by a 250 × 10 array.

To estimate reoccurring dynamic FC patterns (states), we used k-means clustering methods to cluster the 250-window FC matrices for all subjects. We measured the squared Euclidean distance to estimate the similarity between each FC matrix and the cluster centres. The k-means algorithm was iterated 500 times and repeated 150 times on the exemplars of all patients and controls to obtain the group cluster centroids (functional dynamic ECN states). We used the elbow criterion to estimate the optimal number of centroid states (which was determined to be $k = 4$), where each centroid state represented a functional dynamic ECN state.

Then, we examined whether the patients and HCs presented different temporal properties of different functional dynamic ECN states during resting-state fMRI. To count the occurrences of one state, we used only participant data where at least 10 windows belonged to that state. We calculated the following measures in each subject, including: (1) mean dwell time in each state, measured by averaging the number of consecutive windows belonging to one state before changing to another state, which represents how long a subject stayed in a certain state; (2) fractional windows, assessed by the proportion of time spent in each state; and (3) number of transitions, represented state stability over time, and they were measured by the number of times a subject switched from one state to the other. We performed a two-sample *t*-test ($p < 0.05$, FDR corrected) to examine the group differences in mean dwell time and the fractional window in each state and number of transitions between patients and HCs.

Next, we calculated the Pearson correlation between the abnormal temporal properties of dynamic ECN and executive control performance in patients and HCs, respectively, to explore any potential relationship. The correlation analyses were performed using SPSS 16.0 for Windows (SPSS Inc.).

Results

Demographic data and neuropsychological assessment

The patients and HCs did not differ significantly with regard to the age ($t = -0.445$, $p = 0.659$) or educational level ($t = 1.79$, $p = 0.081$). The neuropsychological test results assessed by a two-sample *t*-test are shown in Table 2. The Bonferroni correction was applied for multiple comparisons to reduce the risk of type 1 errors. Hence, a stricter threshold of 0.00625 (0.05/8) as the level of statistical significance was used to explain the results of these two-sample *t*-tests. The patients showed significant impairments in the SDMT ($t = 4.27$, $p = 0.000$) and DST (backward, $t = 4.44$, $p = 0.000$). Uncorrected results showed additional impairments in the Stroop test (dots, $t = -2.44$, $p = 0.019$) and CAVLT (immediate, $t = 3.110$, $p = 0.003$; delayed, $t = 3.356$, $p = 0.002$). However, the scores on SAS ($t = -1.53$, $p = 0.133$) and SDS ($t = -0.81$, $p = 0.425$) were not significantly different between the two groups.

Static functional connectivity of ECN

The five ICs selected as ECNs of interest (Fig. 1) were primarily located in association cortex areas and underwent further analysis of FC changes. IC 3 and IC 15 were

Table 2. Results of cognitive tests of patients and healthy controls.

Item	HCs (mean $\pm$ SD)	Patients (mean $\pm$ SD)	t	p
Age (years)	26.43 $\pm$ 5.22	27.48 $\pm$ 9.49	0.445	0.659
Education (years)	14.65 $\pm$ 1.77	13.52 $\pm$ 2.34	1.79	0.081
SDMT	59.26 $\pm$ 7.57	47.81 $\pm$ 10.13	4.27	0.000*[*]
DST (forward)	9.30 $\pm$ 0.97	8.33 $\pm$ 1.74	2.31	0.026
DST (backward)	7.48 $\pm$ 1.31	5.57 $\pm$ 1.43	4.61	0.000*[*]
Stroop test (colour dot)	12.72 $\pm$ 2.04	14.44 $\pm$ 2.73	$-$2.44	0.019*
Stroop test (colour word)	24.27 $\pm$ 5.96	31.07 $\pm$ 1.26	$-$2.33	0.025
CAVLT (immediate memory following interference)	14.04 $\pm$ 0.82	12.29 $\pm$ 2.57	3.11	0.003*
CAVLT (delayed recall)	13.83 $\pm$ 1.03	11.90 $\pm$ 2.53	3.36	0.002*
CAVLT (recognition)	14.87 $\pm$ ''''0.34	14.43 $\pm$ 0.93	2.13	0.039
SAS	22.09 $\pm$ 2.54	23.33 $\pm$ 2.85	$-$1.53	0.133
SDS	21.91 $\pm$ 3.18	22.61 $\pm$ 2.58	$-$0.81	0.425

DST, Digit Span Test; HCs, healthy controls; SAS, Self-Rating Anxiety Scale; SDMT, Symbol-Digit Modalities Test; SDS, Self-Rating Depression Scale; CAVLT, Chinese auditory verbal learning test.

**[*]*$p < 0.05/8$ (Bonferroni correction).

*[*]$p < 0.05$ (uncorrected results).

mainly located in the prefrontal cortex. IC 3 was mainly located in the ventrolateral prefrontal cortex, whereas IC 15 was mainly located in the dorsolateral prefrontal cortex and medial prefrontal cortex. IC 19, IC 27 and IC 29 were mainly located in frontoparietal association cortex areas: IC 19 and IC 27 were mainly located in the left frontoparietal executive network, whereas IC 29 was mainly located in the right frontoparietal executive network. For the FC between brain regions within the ECN, the results were not significant between the patients and HCs.

Further analysis indicated that, compared to HCs, increased FC was observed between IC 15 and IC 27, IC 15 and IC 29 in patients with anti-NMDA receptor encephalitis (FDR corrected, $p < 0.05$; Table 3 and Fig. 2). Uncorrected results showed increased FC was observed between IC 27 and IC 29 (uncorrected $p < 0.05$; Table 3). Among the patients, when controlling for age, gender and education in a partial correlation, a linear correlation analysis showed a significant positive correlation between IC 15-IC 29 FC and DST (backward) performance ($r = 0.704$, $p = 0.003$, Fig. 3A) and between IC 15-IC 27 FC and SDMT performance ($r = 0.712$, $p = 0.003$, Fig. 3B). No significant correlations between the FC of the ECN and subjects' performances in the DST (forward) test, CAVLT or Stroop test were observed. No significant relationship between static ECN connectivity and cognitive performance was found for HCs.

Temporal properties of dynamic FC state

We identified four patterns of FC states, namely a weaker interconnected state (State 1), a stronger interconnected

Table 3. Results of static functional connectivity among independent components of ECN.

Functional connectivity	t	p
IC 3-IC 15	$-$0.1151	0.9089
IC 3-IC 19	0.0049	0.9961
IC 3-IC 27	0.5391	0.5926
IC 3-IC 29	1.534	0.1325
IC 15-IC 19	$-$0.5958	0.5545
IC 15-IC 27	3.0567	0.0039*
IC 15-IC 29	3.2336	0.0024*
IC 19-IC 27	$-$0.7767	0.4417
IC 19-IC 29	0.2891	0.7739
IC 27-IC 29	2.5718	0.0137*[*]

ECN, executive control network; IC 15, mainly located in the dorsolateral and medial prefrontal cortex; IC 19 and 27, mainly located in the right frontoparietal executive network; IC 29, mainly located in the left frontoparietal executive network; IC 3, mainly located in the ventrolateral prefrontal cortex.

*$p < 0.05$ (FDR corrected).

*[*]$p < 0.05$ (FDR uncorrected).

state (State 2) and two relatively partly stronger interconnected states (States 3 and 4). These four FC states and their corresponding visualized connectivity patterns are shown in Figure 4. Compared to HCs, the patients showed FC was increased between IC 15 and IC 27 in state 3 (FDR corrected, $p < 0.05$; Table 4). Uncorrected results showed increased FC was observed between IC 15 and IC 27 in state 2, between IC 15 and IC 29 in state 3 (uncorrected $p < 0.05$; Table 4). A linear correlation analysis showed no significant correlations between the FC of the ECN and subjects' test performances.

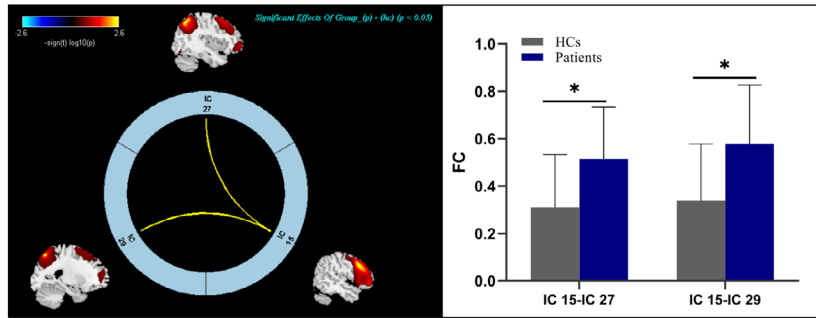Changed dynamic measures derived from the state transition vector were observed in the patients, including

Figure 2. Results of functional connectivity among independent components of ECN. ECN, executive control network; HCs, healthy controls; IC 15, mainly located in the dorsolateral and medial prefrontal cortex; IC 27, mainly located in the right frontoparietal executive network; IC 29, mainly located in the left frontoparietal executive network. *$p < 0.05$ (FDR corrected).
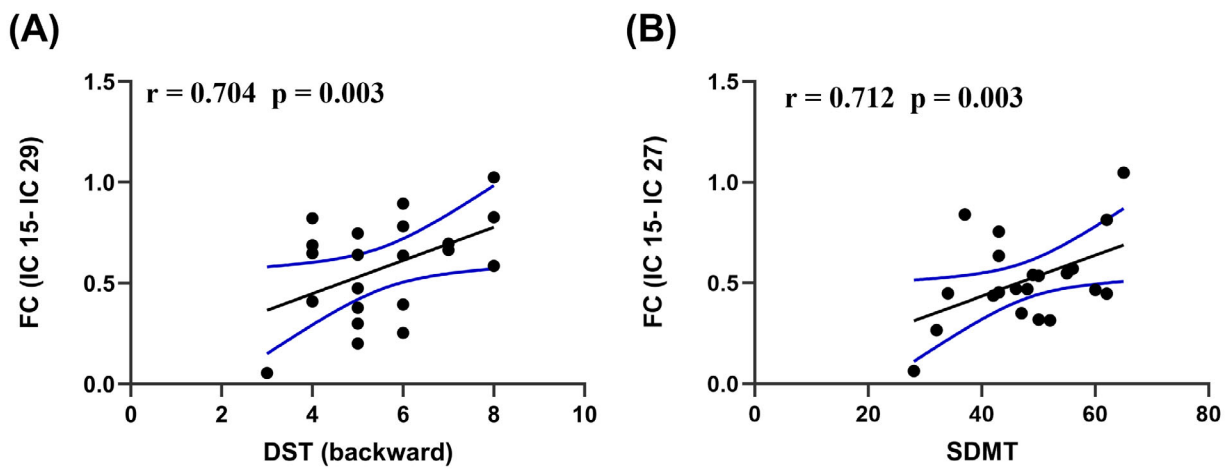

Figure 3. Significant correlations between functional connectivity of two independent components and individual cognitive performance in patients with anti-NMDA receptor encephalitis. (A) symbol-digit modalities test (DST). (B) symbol-digit modalities test (SDMT). IC 15, mainly located in dorsolateral and medial prefrontal cortex; IC 27, mainly located in right fronto-parietal executive network; IC 29, mainly in left fronto-parietal executive network.
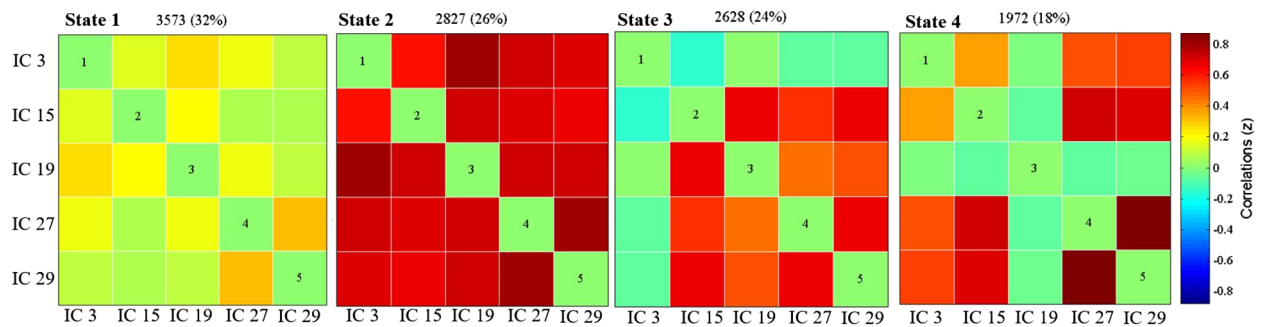

Figure 4. Results of the clustering analysis per state. The total number of occurrences and percentage of total occurrences are listed above each cluster median. IC 3, mainly located in the ventrolateral prefrontal cortex; IC 15, mainly located in the dorsolateral and medial prefrontal cortex; IC 19 and 27, mainly located in the right frontoparietal executive network; IC 29, mainly located in the left frontoparietal executive network.

Table 4. Results of functional connectivity in each state among independent components of ECN.

Functional connectivity	IC 15-IC 27		IC 15-IC 29	
	t	*p*	*t*	*p*
State 1	−1.17	0.2486	−2.50	0.0167**
State 2	−2.89	0.0062**	−1.40	0.1687
State 3	−3.42	0.0015*	−2.46	0.0186**
State 4	−0.84	0.4041	−0.25	0.8014

ECN, executive control network; FDR, false discovery rate; IC 15 = mainly located in the dorsolateral and medial prefrontal cortex, IC 27 = mainly located in the right frontoparietal executive network, IC 29 = mainly located in the left frontoparietal executive network.
*$p < 0.05$ (FDR corrected).
**$p < 0.05$ (FDR uncorrected).

both mean dwell time and fractional windows. The mean dwell time in State 1 was significantly shorter in patients with anti-NMDA receptor encephalitis than in HCs ($t = 2.7043$, $p = 0.0098$) (Fig. 5A). There was no significant difference between the two groups regarding the mean dwell time in State 2 ($t = -1.1594$, $p = 0.2529$), State 3 ($t = -0.2321$, $p = 0.8176$) and State 4 ($t = -1.2881$, $p = 0.2048$) (Fig. 5A). Similarly, the fractional windows in State 1 were significantly lower in patients with anti-NMDA receptor encephalitis than in HCs ($t = 2.493$, $p = 0.017$) (Fig. 5B). Correspondingly, the fractional windows of patients with anti-NMDA receptor encephalitis in State 4 were significantly higher than in HCs ($t = -2.177$, $p = 0.035$) (Fig. 5B). There was no significant difference between the two groups regarding the fractional windows in State 2 ($t = -0.640$, $p = 0.526$) and State 3 ($t = -0.014$, $p = 0.989$) (Fig. 5B). Regarding the number of transitions, no significant differences were found with respect to the number of transitions between states ($t = -0.133$, $p = 0.895$). Overall, these changes indicated that in patients with anti-NMDA

receptor encephalitis, the stability of the weaker within-ECN FC (State 1) was significantly affected.

Among the patients, when controlling for age, gender and education in a partial correlation, we found that the fractional windows in State 1 were negatively correlated with DST (backward) performance ($r = -0.597$, $p = 0.019$, Fig. 6A) and positively correlated with the Stroop test (colour-word: $r = 0.643$, $p = 0.010$, Fig. 6B). We also observed a negative correlation trend with DST (forward) performance ($r = -0.508$, $p = 0.053$) for the fractional windows in State 1. There were no significant correlations between the fractional windows in State 1 and SDMT or CAVLT. For the fractional windows in State 4 and the mean dwell time in State 1, no significant correlations with cognitive performance were observed. No significant relationship between dynamic ECN alterations and cognitive performance was found for HCs.

Discussion

To our knowledge, this study is the first to investigate the association between cognitive function impairments and abnormal static and dynamic metrics of ECN in a cohort of patients with anti-NMDA receptor encephalitis past the acute stage. Our study revealed the following findings: (1) patients with anti-NMDA receptor encephalitis past the acute stage showed significant cognitive function impairments compared to HCs; (2) static intrinsic FC of ECN alterations was found in the patients; (3) changed dynamic metrics were observed in the patients, including mean dwell time and fraction of time spent in certain states; and (4) significant correlations between altered metrics of ECN and cognitive performance were observed in the patients. These results provide evidence that static and dynamic ECN alterations may be related to cognitive function impairments in anti-NMDA receptor encephalitis, which sheds new light on the pathophysiological mechanisms underlying this disease.
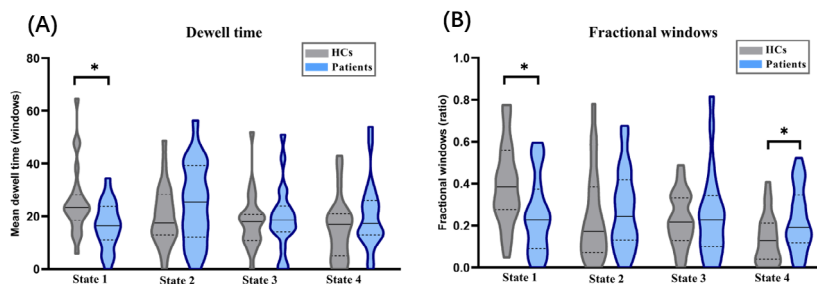

Figure 5. Temporal properties of dynamic functional connectivity states for the anti-NMDA receptor encephalitis and healthy control groups. (A) Mean dwell time. (B) the fractional windows were plotted using violin plots. Horizontal lines indicate group medians and interquartile range (solid and dashed line, respectively). HCs = healthy controls. *$p < 0.05$.
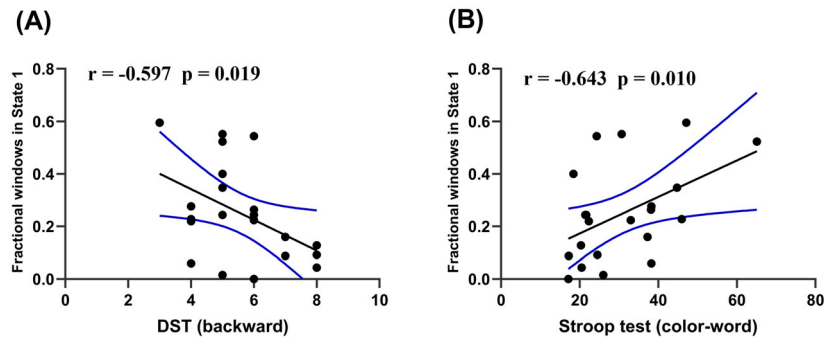
(A)

r = -0.597 p = 0.019

(B)

r = -0.643 p = 0.010

Figure 6. Significant correlations between fractional windows in State 1 and individual performance of DST (A), Stroop test (B) in patients with anti-NMDA receptor encephalitis. DST, digit span test; anti-NMDA, anti-*N*-methyl-ᴅ-aspartate.

As expected, our study demonstrated that patients with anti-NMDA receptor encephalitis past the acute stage possess persistent cognitive function impairments, especially working memory deficits and information processing speed impairments, based on their performances on neuropsychological tests. These results are consistent with those in previous studies, which showed that cognitive function impairments of varying degrees may persist for a lifetime in these patients.[4,5] It was suggested that early immunotherapy should be uniformly and consistently considered to produce favourable cognitive outcomes[4,5]; however, a retrospective study showed that working memory, information processing speed and executive function impairments of various degrees may persist for a lifetime in moderate-to-severe patients despite aggressive treatment applications.[6]

It is increasingly clear that anti-NMDA receptor encephalitis results not only in alterations in the default-mode network (DMN) supporting episodic memory processing but also in frontoparietal networks supporting schizophrenia-like symptoms.[13] These latter networks are anatomically related to regions of executive control function. Consistent with a previous study,[13] the static functional network connectivity results in patients with anti-NMDA receptor encephalitis showing altered patterns of FC within the ECN, including increased FC between the prefrontal portions of the ECN (dorsolateral and medial) and frontoparietal executive networks. In addition, in patients with anti-NMDA receptor encephalitis, alterations in the ECN were positively related to DST (backward) and SDMT performance. Extending the previous observation of impaired frontoparietal networks,[13] our data support the idea that ECN dysfunction is related to difficulties in top-down regulation in this disease past the acute stage. This idea is in line with evidence that these cognitive function impairments may be associated with disorganized patterns of neuronal activity in the ECN, which has also been observed in other psychiatric disorders, such as schizophrenia.[34]

Aside from altered static FC in the ECN, we also investigated whether dynamic FC and the temporal properties of the ECN were abnormal in anti-NMDA receptor encephalitis. Dynamic FC may embody features of neural system functional capacity and could act as a potential disease biomarker.[15,16] Our results indicated four discrete connectivity configurations, a weaker interconnected State 1, a stronger interconnected State 2, and two relatively partly stronger interconnected States 3 and 4. However, we were only able to replicate increased FC between the prefrontal portions of ECN (dorsolateral and medial) and right frontoparietal executive network in one of the four connectivity stats. The reasons for this may be as follows. First, we obtained static FC by calculating FC within the entire scanning period and used a measure of average FC across the four dynamic states. Second, the FC patterns between State 3 and the static FC were highly similar based on the spatial correlation between the cluster centroid of each state and the static FC matrix. The limited evidence of dynamic FC abnormalities may very well be a more comprehensive explanation of FC alterations when compared with static FC analyses that "oversimplify" the data based on the static time course hypothesis.[15,35]

In this study, we also conducted an exploratory analysis to examine the dynamic metrics derived from state vectors. Interestingly, the results showed that overall, patients with anti-NMDA receptor encephalitis have significantly different temporal properties of dynamic FC states than those of HCs. The patients' dwell times were shorter in the weaker interconnected State 1 and they had lower fractional windows in the weaker interconnected State 1, indicating that the stability of the weaker within-ECN FC (State 1) was significantly affected in this population. Correspondingly, the fractional windows of patients in the partly stronger interconnected State 4 were significantly higher than those of HCs. Dwell time abnormalities may be associated with disorganized neuronal activity patterns, which has also been observed in other neurological and psychiatric disorders, such as Alzheimer's disease,[21] Parkinson's disease,[36] epilepsy[20] and schizophrenia.[16,37] Our findings lead us to suggest that patients with anti-NMDA receptor encephalitis are unable to remain in the weaker within-ECN FC (State 1) for extended periods of time due to these disorganized neuronal activity patterns.

In addition, the temporal properties were significantly related to cognitive performance (DST (backward) and Stroop tests). It should be noted that high scores in the Stroop test represent poor executive control performance, hence, worsening of executive control performance correlated with higher State 1 proportion in the fractional windows. In other words, in this weaker interconnected state (State 1), the efficiency of executive control processing may be low in patients with anti-NMDA receptor encephalitis past the acute stage. Taken together, these results may provide evidence of the vulnerability of the resting-state ECN in anti-NMDA receptor encephalitis with executive control function impairments and underline the importance of further investigating the relationship of this disease-related cognitive signature to the temporal dynamics of FC. It is noteworthy that these results are not discernible through static FC analyses, which suggests the value of using dynamic FC to accurately understand the pathophysiological mechanism in anti-NMDA receptor encephalitis. Studies have shown that abnormalities in both static and dynamic connectivity metrics could indicate the complementary nature of these two FC analyses.[35,38] Based on this information, future studies would benefit from using both static and dynamic FC analyses to explore the neurophysiological mechanisms.[35]

This study had a few limitations that should be considered. First, although our findings suggested that the abnormal static and dynamic FC in the ECN might be associated with cognitive performance, the mechanism by which these alterations in the ECN influence cognitive function processing is still unknown. Our hypothesis could be strengthened by conducting static and dynamic FC analyses on task-related fMRI data to specifically investigate cognitive function processing. Second, all the recruited patients in this study were past the acute stage; thus, it remains unclear how cognitive function might be influenced by selective NMDA receptor disruption at earlier stages. Further longitudinal studies covering more stages are needed to gain deeper insight into the neural mechanisms underlying cognitive function deficits in anti-NMDA receptor encephalitis.

In summary, results from this study suggest that altered static and dynamic ECN connectivity may affect cognitive function in patients with anti-NMDA receptor encephalitis past the acute stage. These findings may provide a new perspective to the pathophysiological mechanisms underlying cognitive function in this population.

Acknowledgements

Author Contributions

Study concept and design: K. Wang, Z. Q. Chen and J. T. Zhou; data acquisition, analysis and interpretation: all authors; drafting of the manuscript: K. Wang, Z. Q. Chen and J. T. Zhou; critical review of manuscript: all authors.

Conflicts of Interest

None of the authors have potential conflicts of interest to be disclosed.

References

1. Dalmau J, Gleichman AJ, Hughes EG, et al. Anti-NMDA-receptor encephalitis: case series and analysis of the effects of antibodies. Lancet Neurol. 2008;7(12):1091-1098.

2. Dalmau J, Lancaster E, Martinez-Hernandez E, Rosenfeld MR, Balice-Gordon R. Clinical experience and laboratory investigations in patients with anti-NMDAR encephalitis. Lancet Neurol. 2011;10(1):63-74.

3. Titulaer MJ, McCracken L, Gabilondo I, et al. Treatment and prognostic factors for long-term outcome in patients with anti-NMDA receptor encephalitis: an observational cohort study. Lancet Neurol. 2013;12(2):157-165.

4. McKeon GL, Robinson GA, Ryan AE, et al. Cognitive outcomes following anti-N-methyl-D-aspartate receptor encephalitis: a systematic review. J Clin Exp Neuropsychol. 2018;40(3):234-252.

5. Finke C, Kopp UA, Pruss H, Dalmau J, Wandinger KP, Ploner CJ. Cognitive deficits following anti-NMDA receptor encephalitis. J Neurol Neurosurg Psychiatry. 2012;83(2):195-198.

6. Wang K, Chen Z, Wu D, et al. Early second-line therapy is associated with improved episodic memory in anti-NMDA receptor encephalitis. Ann Clin Transl Neurol. 2019;6 (7):1202-1213.

7. Caciagli L, Wandschneider B, Xiao F, et al. Abnormal hippocampal structure and function in juvenile myoclonic epilepsy and unaffected siblings. Brain. 2019;142(9):2670-2687.

8. Sala-Llonch R, Bosch B, Arenaza-Urquijo EM, et al. Greater default-mode network abnormalities compared to high order visual processing systems in amnestic mild cognitive impairment: an integrated multi-modal MRI study. J Alzheimers Dis. 2010;22(2):523-539.

9. Xie Y, Cui Z, Zhang Z, et al. Identification of amnestic mild cognitive impairment using multi-modal brain features: a combined structural MRI and diffusion tensor imaging study. J Alzheimers Dis. 2015;47(2):509-522.

10. Curtis CE, D'Esposito M. Persistent activity in the prefrontal cortex during working memory. Trends Cogn Sci. 2003;7(9):415-423.

11. Ridderinkhof KR, van den Wildenberg WP, Segalowitz SJ, Carter CS. Neurocognitive mechanisms of cognitive control: the role of prefrontal cortex in action selection, response inhibition, performance monitoring, and reward-based learning. Brain Cogn. 2004;56(2):129-140.

12. Silva PHR, Spedo CT, Baldassarini CR, et al. Brain functional and effective connectivity underlying the information processing speed assessed by the Symbol Digit Modalities Test. Neuroimage. 2019;184:761-770.

13. Peer M, Pruss H, Ben-Dayan I, Paul F, Arzy S, Finke C. Functional connectivity of large-scale brain networks in patients with anti-NMDA receptor encephalitis: an observational study. Lancet Psychiatry. 2017;4(10):768-774.

14. Kucyi A, Davis KD. Dynamic functional connectivity of the default mode network tracks daydreaming. Neuroimage. 2014;100:471-480.

15. Hutchison RM, Womelsdorf T, Allen EA, et al. Dynamic functional connectivity: promise, issues, and interpretations. Neuroimage. 2013;80:360-378.

16. Damaraju E, Allen EA, Belger A, et al. Dynamic functional connectivity analysis reveals transient states of dysconnectivity in schizophrenia. Neuroimage Clin. 2014;5:298-308.

17. Demirtas M, Tornador C, Falcon C, et al. Dynamic functional connectivity reveals altered variability in functional connectivity among patients with major depressive disorder. Hum Brain Mapp. 2016;37(8):2918-2930.

18. Marusak HA, Calhoun VD, Brown S, et al. Dynamic functional connectivity of neurocognitive networks in children. Hum Brain Mapp. 2017;38(1):97-108.

19. Liao W, Zhang Z, Mantini D, et al. Dynamical intrinsic functional architecture of the brain during absence seizures. Brain Struct Funct. 2014;219(6):2001-2015.

20. Liu F, Wang Y, Li M, et al. Dynamic functional network connectivity in idiopathic generalized epilepsy with generalized tonic-clonic seizure. Hum Brain Mapp. 2017;38(2):957-973.

21. Jones DT, Vemuri P, Murphy MC, et al. Non-stationarity in the "resting brain's" modular architecture. PLoS One. 2012;7(6):e39731.

22. Kim J, Criaud M, Cho SS, et al. Abnormal intrinsic brain functional network dynamics in Parkinson's disease. Brain. 2017;140(11):2955-2967.

23. Du Y, Pearlson GD, Yu Q, et al. Interaction among subsystems within default mode network diminished in schizophrenia patients: a dynamic connectivity approach. Schizophr Res. 2016;170(1):55-65.

24. Yao Z, Hu B, Xie Y, et al. Resting-state time-varying analysis reveals aberrant variations of functional connectivity in autism. Front Hum Neurosci. 2016;10:463.

25. Graus F, Titulaer MJ, Balu R, et al. A clinical approach to diagnosis of autoimmune encephalitis. Lancet Neurol. 2016;15(4):391-404.

26. Wang J, Wang X, Xia M, Liao X, Evans A, He Y. GRETNA: a graph theoretical network analysis toolbox for imaging connectomics. Front Hum Neurosci. 2015;9:386.

27. Calhoun VD, Adali T, Pearlson GD, Pekar JJ. A method for making group inferences from functional MRI data using independent component analysis. Hum Brain Mapp. 2001;14(3):140-151.

28. Li YO, Adali T, Calhoun VD. Estimating the number of independent components for functional magnetic resonance imaging data. Hum Brain Mapp. 2007;28 (11):1251-1266.

29. Himberg J, Hyvarinen A, Esposito F. Validating the independent components of neuroimaging time series via clustering and visualization. Neuroimage. 2004;22(3):1214-1222.

30. Du Y, Fan Y. Group information guided ICA for fMRI data analysis. Neuroimage. 2013;69:157-197.

31. Smith SM, Fox PT, Miller KL, et al. Correspondence of the brain's functional architecture during activation and rest. Proc Natl Acad Sci USA. 2009;106(31):13040-13045.

32. Zuo XN, Kelly C, Adelstein JS, Klein DF, Castellanos FX, Milham MP. Reliable intrinsic connectivity networks: test-retest evaluation using ICA and dual regression approach. Neuroimage. 2010;49(3):2163-2177.

33. Allen EA, Damaraju E, Plis SM, Erhardt EB, Eichele T, Calhoun VD. Tracking whole-brain connectivity dynamics in the resting state. Cereb Cortex. 2014;24(3):663-676.

34. Minzenberg MJ, Laird AR, Thelen S, Carter CS, Glahn DC. Meta-analysis of 41 functional neuroimaging studies of executive function in schizophrenia. Arch Gen Psychiatry. 2009;66(8):811-822.

35. Calhoun VD, Miller R, Pearlson G, Adali T. The chronnectome: time-varying connectivity networks as the next frontier in fMRI data discovery. Neuron. 2014;84 (2):262-274.

36. Fiorenzato E, Strafella AP, Kim J, et al. Dynamic functional connectivity changes associated with dementia in Parkinson's disease. Brain. 2019;142(9):2860-2872.

37. Lottman KK, Kraguljac NV, White DM, et al. Risperidone effects on brain dynamic connectivity-a prospective resting-state fMRI Study in schizophrenia. Front Psychiatry. 2017;8:14.

Supporting Information

Additional supporting information may be found online in the Supporting Information section at the end of the article.

Figure S1. An overview of analysis steps of static and dynamic of executive control network.